PHOTONICS Research

High-Q surface electromagnetic wave resonance excitation in magnetophotonic crystals for supersensitive detection of weak light absorption in near-infrared

O. V. Borovkova,[1,*] D. O. Ignatyeva,[1,2] S. K. Sekatskii,[3] A. Karabchevsky,[4,5] and V. I. Belotelov[1,2]

[1]Russian Quantum Center, Skolkovo, Moscow 143025, Russia
[2]Lomonosov Moscow State University, Moscow 119991, Russia
[3]Laboratoire de Physique de la Matière Vivante, IPHYS, EPFL, 1015 Lausanne, Switzerland
[4]School of Electrical and Computer Engineering, Ben-Gurion University of the Negev, Beer-Sheva 8410501, Israel
[5]e-mail: alinak@bgu.ac.il
*Corresponding author: o.borovkova@rqc.ru

Received 20 August 2019; revised 15 November 2019; accepted 16 November 2019; posted 19 November 2019 (Doc. ID 375736); published 19 December 2019

The mid-infrared spectrum can be recorded from almost any material, making mid-infrared spectroscopy an extremely important and widely used sample characterization and analysis technique. However, sensitive photoconductive detectors operate primarily in the near-infrared (NIR), but not in the mid-infrared, making the NIR more favorable for accurate spectral analysis. Although the absorption cross section of vibrational modes in the NIR is orders of magnitude smaller compared to the fundamental vibrations in the mid-infrared, different concepts have been proposed to increase the detectability of weak molecular transitions overtones. Yet, the contribution of magnetophotonic structures in the NIR absorption effect has never been explored so far. Here we propose high-Q magnetophotonic structures for a supersensitive detection of weak absorption resonances in the NIR. We analyze the contributions of both magnetic and nonmagnetic photonic crystal configurations to the detection of weak molecular transitions overtones. Our results constitute an important step towards the development of highly sensitive spectroscopic tools based on high-Q magnetophotonic sensors.

https://doi.org/10.1364/PRJ.8.000057

1. INTRODUCTION

Absorption spectroscopy in the mid-infrared (mid-IR) range is widely used to investigate and detect organic molecules [1]. This technique allows detecting molecules in mixtures of substances without prior separation but rather due to the well-defined spectral lines associated with fundamental vibrations. Spectral analysis is particularly important for fixing minor changes in the composition of proteins by studying the fingerprints (identification) of molecular bonds—for instance, the peptide bonds in proteins [2,3]. However, highly sensitive photoconductive detectors function in the near-infrared (NIR) but not in the mid-IR. Also, affordable materials, such as glass and quartz, are transparent for NIR radiation and thus can be used to make cell windows, focusing lenses, and optical fibers.

The circumstance that the absorption cross sections of the higher harmonics of vibrational transitions are several orders of magnitude smaller than those of the fundamental transitions and have a low signal-to-noise ratio (SNR) in the absorption spectrum, makes it difficult to use absorption spectroscopy methods in the NIR range for the identification of molecules. Recently, Karabchevsky and her group proposed exploring the high-order vibrational transitions (overtones) lying in the NIR range on glass waveguides [4]. Earlier, giant absorption of light was observed and explained as a switch from the ballistic to the diffusive regime in borosilicate waveguides [4] and silicate microfibers [5]. Several concepts were proposed to explore the interaction of electromagnetic radiation with overtone transitions, which are forbidden transitions in the dipole approximation, such as, e.g., the glass waveguide described above, silicon (Si) rib waveguides [6], and planar and cylindrical waveguides [7]. One of the most promising methods to increase the sensitivity of the infrared absorption spectroscopy is the two orders of magnitude amplification of the electric field when the plasmon resonances are excited [8–12].

High sensitivity of the surface plasmon resonance (SPR) to the refractive index of the external medium underlies widely

used SPR-based sensors [13,14], which detect the smallest variations of the refractive index of analyzed substances as the shift of the optical resonance associated with surface plasmon polariton (SPP) excitation. However, SPP on a smooth metal surface provides a rather low-quality (Q) factor resonance so there are many opportunities for system improvement. For example, optical resonances in nanostructured plasmonic materials [10–12] are shown to be useful for sensing applications. However, utilization of such complex structures is challenging, so another option is to design the layered structure with high-Q resonance.

As has been demonstrated earlier, the plasmonic structures exhibit a very high sensitivity to the small nonlinear and gyrotropic components of the permittivity tensor [15–17]. This gives rise to several orders of enhancement of the magneto-optical (MO) effects in magnetoplasmonic structures [18–21]. The MO response, i.e., magnetic-field-induced light polarization rotation or intensity modulation, enhanced by several orders of magnitude near the resonance, is more sensitive than the reflectance spectra measured in nonmagnetic SPR sensors. Therefore, a significant improvement of sensitivity and the resolution of MO surface resonance-based sensors, as well as the SNR was achieved by utilization of the magnetic layers in a plasmonic structure [22–27].

However, a physical limit of SPR sensing is associated with the low Q factor arising from light absorption by metals. Ferromagnetic metals or dielectrics possess even higher losses than nonmagnetic ones. In traditional sensors, where the variations of the real part of the refractive index are measured, utilization of all-dielectric structures supporting high-quality quasi-surface wave resonances instead of plasmonic structures increases the SNR and sensitivity by an order of magnitude [28,29]. Even higher sensitivity was demonstrated for the magnetophotonic structures where the ultrahigh Q factor MO resonances are excited [29–33].

In this paper, for what we believe is the first time, we propose the utilization of all-dielectric magnetophotonic structures for sensing of the imaginary part of the permittivity having very weak resonances in the NIR. We show that excitation of high-Q resonances of the quasi-surface waves in the all-dielectric structures is promising for measurements of the vibrational transitions of organic molecules for several reasons. First, the small absorption peaks of the studied substances in the NIR are the only source of absorption in all-dielectric transparent structures. Therefore, the high-Q of the resonances is responsible for a large sensitivity to the losses produced by the absorption peaks. Then, the MO Kerr effect is known [34] to depend significantly on the structure absorption. Thus, even the minute peaks in the analyzed molecules' absorption spectra that refer to the higher harmonics of the vibrational transitions could be efficiently detected. We would like to point out that the influence of magnetic fields on a weak absorption by molecular transitions overtones has not been studied before.

Here, we propose two photonic crystal (PC)-based nanostructures for very high-Q sensing of N-methylacetamide (NMA) molecules. Both structures provide narrow resonances in the reflection spectrum, corresponding to the absorption peaks typical for NMA molecules [4,7]. This allows one to detect the presence of NMA molecules in an analyte with high sensitivity. The first PC nanostructure is nonmagnetic and includes just four pairs of silicon/silicon nitride (Si_3N_4) layers and an additional Si layer. The nanostructure demonstrates an ultranarrow resonance dip in reflectance associated with a small absorption peak while illuminated by s-polarized light. It is worth noting that this structure is simple in terms of fabrication due to the small number of layers. The second structure provides more sensitive detection due to the narrower magnetophotonic resonance in comparison with the nonmagnetic PC nanostructure.

2. ULTRALONG-PROPAGATION QUASI-SURFACE MODES FOR ABSORPTION PEAK DETECTION

The sensing concept is schematically depicted in Fig. 1. The multilayered stack of the PC nanostructure is placed on a prism and illuminated by a focused broadband light beam. We designed the PC structures to support the excitation of the long-range propagating quasi-surface electromagnetic modes. The excited mode represents a guiding mode localized in the terminating layer of the PC structure due to the PC bandgap (BG) on the one side and total internal reflection on the other.

The parameters of the PC are tuned so that under near-cutoff conditions, it has a strongly asymmetric profile with large penetration depth to the analyzed substance and therefore exhibits high sensitivity to analyte permittivity. Although the excited mode is guided by its nature, its field distribution and sensitivity are very similar to surface plasmon polariton modes, so this mode is referred to as a "quasi-surface." Such types of modes were shown [28–30] to combine the advantages of the guided modes—such as large Q, and surface modes—such as large penetration depth and high sensitivity to the optical properties of the external medium. Note that the Q factor is a key point for sensing: structures with a low Q factor have high losses themselves and provide very small light–matter interaction, and therefore are not suitable for sensing.

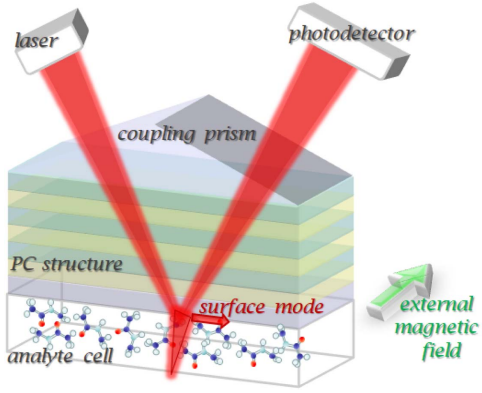

Fig. 1. Schematic representation of the proposed sensor. Incident light illuminates the prism, which in turn provides the momentum to excite the quasi-surface modes. The surface modes excite the studied organic molecular vibrations overtones in the PC-based multilayer sensor that is observed in the reflectance spectra of s-polarized light for the nonmagnetic structure and in the transverse MO Kerr effect spectra of p-polarized light for the magnetic structure.

The spectral position of this mode resonance is tuned to overlap with spectral resonances of the overtone transitions of the studied analyte molecules. We have selected NMA as an analyzed substance since it exhibits a very small absorption peak with the extinction coefficient of $n'' = 10^{-4}$ at a wavelength of 1.495 μm [4,7]. We should note that the excited surface mode in an all-dielectric lossless transparent structure is very sensitive to the small absorption peaks arising from the vibration overtones of molecules since it is the only source of absorption in the structure (in contrast to the plasmonic structures). The presence of the absorption at the peculiar frequencies results in the appearance of the corresponding narrow dips in the reflectance spectra of the PC-based sensor totally vanishing if the absorption is set to zero. Thus, the PC-based structure provides an efficient method for small absorption peaks measurement.

Further improvement of the discussed structure could be performed if the terminating (guiding) layer of the PC-based structure is magnetic. In this case, the transversal MO Kerr effect δ_R (TMOKE) could be observed in reflection as the relative change of the reflection coefficient of the PC nanostructure R when the structure is remagnetized in opposite directions ($+M$ and $-M$) via an external magnetic field [28],

$$\delta_R = \Delta R/R = 2[R(M) - R(-M)]/[R(M) + R(-M)]. \quad \textbf{(1)}$$

Here we denote the absolute change of the reflection coefficient R when the structure is remagnetized as $\Delta R = R(M) - R(-M)$. TMOKE is significantly enhanced near the excited resonance dip in reflectance, providing even higher Q and a more sensitive tool for the tracking of the small absorption peaks.

3. ULTRAHIGH-Q RESONANCE IN NONMAGNETIC PC-BASED STRUCTURE

In order to excite the quasi-surface electromagnetic mode at the PC–analyte interface, we designed the PC-based structure, which consists of four pairs of layers of Si_3N_4 with a thickness of 222 nm and Si with a thickness of 135 nm, while the thickness of the bottom Si layer is 260 nm. The thickness of the bottom Si layer h determines both an angular position and the Q factor of the resonance in the reflection spectra, so that $h = 260$ nm provides the balance between the quality of the resonance and the typical tolerance of the fabrication process about several nanometers (see Appendix A). The PC structure and the electromagnetic field distribution are shown in Fig. 2(a). The proposed design of the PC nonmagnetic sensor provides the TE-polarized surface mode at 1.495 μm with the evanescent field penetrating into the analyte (NMA). The s-polarized light illuminates the facet of the Si equilateral prism with angle of 27° to the PC surface normal. Although a center of the photonic BG in the angular spectrum of the PC is at 27° [Fig. 2(b)], due to the finite thickness of the PC, the light partially goes through the PC to the bottom Si layer.

Figure 2(b) shows the reflectance at the incident angle versus wavelength spectrum in the non-magnetic sensor configuration. Ultranarrow resonance [also shown in Fig. 2(c) in the magnified scale] is in the BG of the PC structure and also below the total internal reflection line ($\theta = 26.65°$). Therefore, the

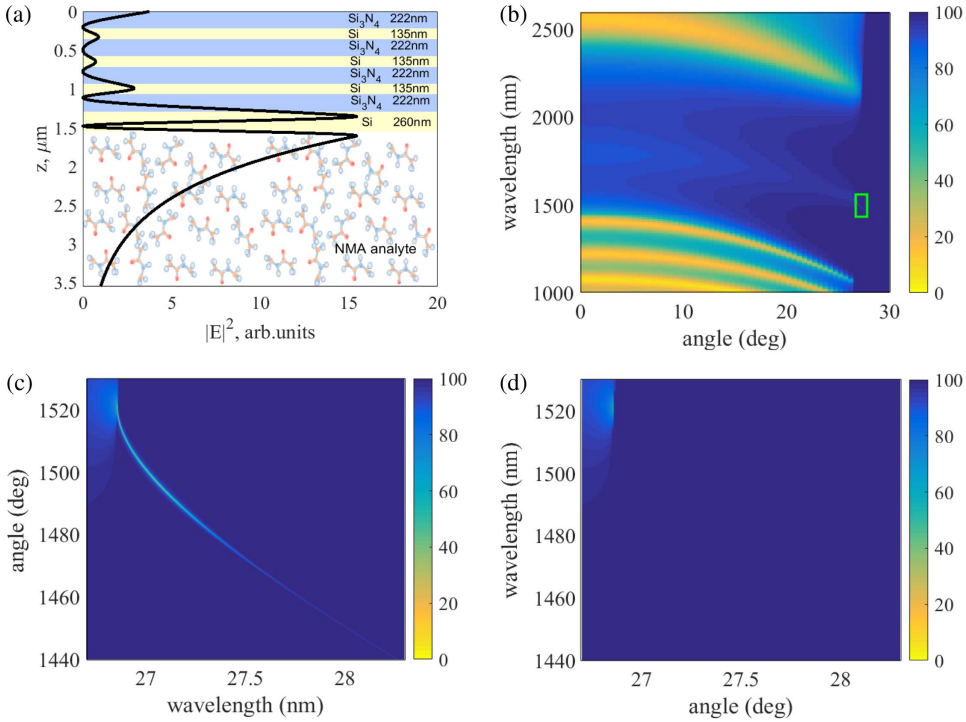

Fig. 2. (a) PC structure scheme and the electromagnetic field distribution of the mode inside the PC structure and NMA analyte. The reflectance spectrum (incidence angle versus wavelength) of the PC-based structure for superhigh Q sensing; (b) large scale, the position of the excited mode with respect to the PC BG and total internal reflection angle, shown by green rectangle; (c) magnified scale showing the ultrahigh-Q of the excited mode; (d) magnified scale showing the disappearance of the resonance in the case of zero absorption.

designed structure provides the waveguide propagation of light inside the structure due to the total internal reflection from the analyte on the one side, and a photonic BG on the other side. The structure is designed to establish the near-cutoff conditions, so that the light intensity distribution inside this bottom waveguide Si layer and in the neighboring regions is highly asymmetric and efficiently penetrates inside the analyte; see Fig. 2(a).

The bright curve in Fig. 2(c) depicts the position of the resonance associated with the weak absorption peaks of NMA molecules. One can see that the proposed design guarantees the existence of the high-Q resonance with $Q = 1670$ in the spectral range from 1.48 to 1.52 μm, which coincides with the NMA absorption line of the N-H vibrational mode. At shorter wavelengths the addressed resonance becomes shallow and gradually disappears. Therefore, even a weak absorption peak at 1.495 μm with an extinction coefficient as small as $n'' = 10^{-4}$ (typical of the NMA molecules) causes a noticeable dip in the reflection spectra of light at an angle of incidence of 27.1°.

In order to reveal the impact of small extinction resonance of the studied molecules on the reflectance resonance, we have numerically compared the optical response of the sensing structure in two cases, with [$n'' = 10^{-4}$, Fig. 2(c)] and without [$n'' = 0$, Fig. 2(d)] absorption of the analyte. If we set the extinction coefficient of the analyte to zero and leave all other parameters and dielectric properties, including refraction indices of the materials, unchanged, the resonance in the reflection spectra clearly seen in Fig. 2(c) disappears in Fig. 2(d). The absence of the resonance in Fig. 2(d) shows that the resonant dip in the reflection emerges due to the absorption properties of the NMA molecules. This behavior is explained by the coupled back radiation into the reflected light, which in lossless structure is 100% (see Appendix C). This is a key point for the addressed sensor of the NMA molecules.

4. ULTRANARROW MO RESONANCE IN THE PC-BASED MAGNETIC NANOSTRUCTURE

An important feature of the MO effects is the fact that they are strongly dependent on the dielectric properties of materials, including absorption. Moreover, it has been reported earlier that even minute changes of the permittivity tensor could be sufficient for the perceptible changes in the MO effects spectra in specially designed structures providing a novel approach to optical sensing [18,29,30]. Usually, the MO sensing structures utilize TMOKE.

This MO effect appears only for p-polarized light; thus, in contrast to the non-magnetic PC nanostructure, here we tune the PC parameters to excite a TM-type mode. The PC consisting of 20 pairs of Ta_2O_5 (255 nm)/Si (373 nm) layers is terminated with magnetic cerium-substituted yttrium iron-garnet (CeYIG), deposited to provide MO response. The PC nanostructure under consideration is placed inside the reversible magnetic field directed along the plane of the PC layers and

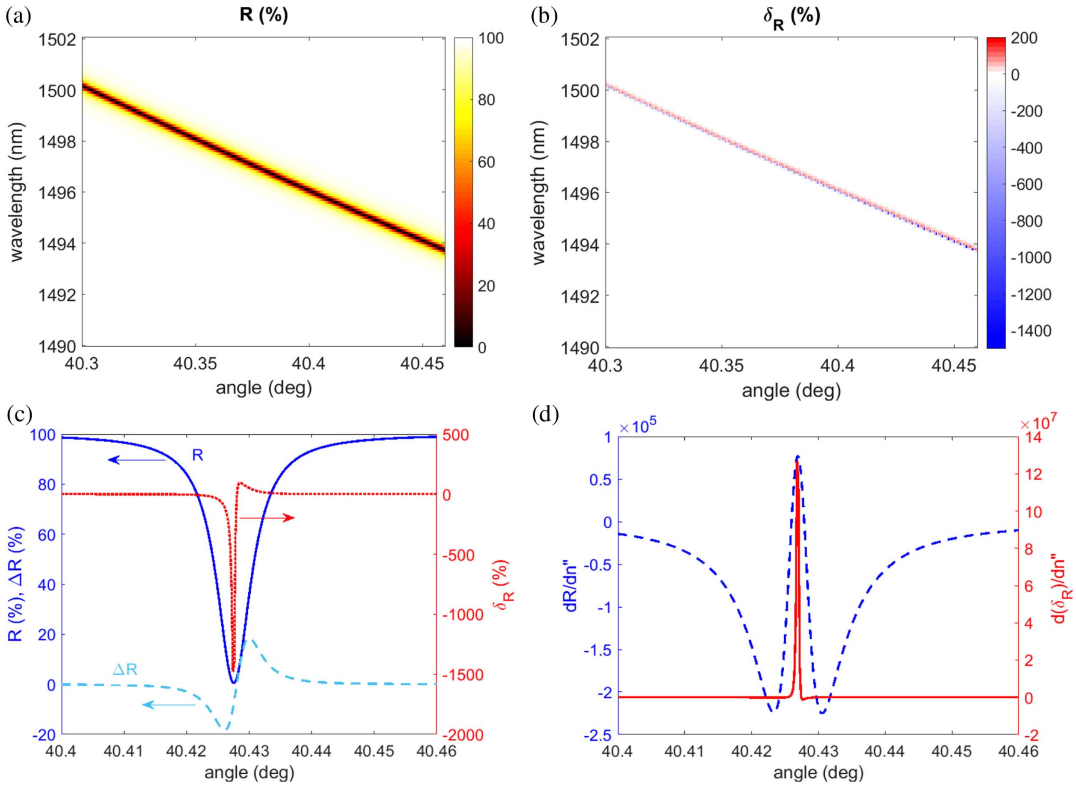

Fig. 3. Magnetic sensing structure with TM-polarized quasi-surface mode. (a) Reflectance (R) and (b) TMOKE magnified scale wavelength versus angle plot showing the ultrahigh-Q of the excited mode and corresponding enhancement of the MO response; (c) R (solid line), ΔR (dashed line), and TMOKE δ_R (dotted line) angular spectra at the resonance wavelength 1.495 μm; (d) angular spectra of sensitivity of optical and MO response to the extinction coefficient of the analyte, dR/dn'' and $d(dR/R)/dn''$.

orthogonally to the incident light wave vector. The scheme of the addressed nanostructure and the applied magnetic field H are given in Figs. 1 and 7 (in Appendix C). One of the equilateral TiO_2 prism side facets is illuminated by p-polarized light. The reflected light is detected on the other side facet of the prism.

The proposed design of the PC nanostructure demonstrates narrow optical resonance at the wavelength 1.495 μm for the incident angle of 40.43° [Fig. 3(a)]. This resonance is related to the excitation of the TM-type quasi-surface mode. The applied external magnetic field affects that mode and thereby changes the optical response of the structure. As a result, the resonant enhancement of TMOKE is observed [Fig. 3(b)].

Let us analyze in detail how the reflectance spectra, ΔR, and TMOKE, δ_R, behave in the presence of a weakly absorbing medium, the NMA molecules in this case. The angular spectra of R, ΔR and a ratio δ_R are given in Fig. 3(c). One can see that the designed structure has a clear dip in the reflectance spectrum. The width of the resonance in ΔR spectrum is comparable with the resonance in the reflectance spectrum. However, the resonance in the TMOKE spectrum, δ_R, is significantly narrower and has a higher Q factor: $Q_R = 5.82 \times 10^3$, $Q_\delta = 7.87 \times 10^4$. An increase in the Q factor by one order allows us to speak with confidence about a significant increase in the sensitivity of the method based on measuring the MO effect as compared with the approach based on measuring the reflection spectrum.

This feature of the TMOKE resonance was earlier reported to enhance the sensitivity of the sensors measuring the changes of the real part of the medium refractive index. We argue that high Q factor of the TMOKE resonance together with the enhanced magnitude up to 1000% is also responsible for the amplification of the sensitivity to the imaginary part of the medium refractive index. Therefore, the small absorption peaks of the material in the NIR could be detected and the presence of the NMA molecules in the analyte could be measured with greater precision.

Figure 3 shows the sensitivity of the reflectance and TMOKE spectra to the variation of the extinction coefficient. The dramatic increase of the MO sensitivity of more than one order of magnitude compared to the sensitivity of the optical sensor is clearly observed near the resonance of the quasi-surface electromagnetic mode.

5. DISCUSSION

To conclude, we have theoretically explored for the first time the MO effects on the molecular vibrational overtones in the NIR. We proposed two types of the PC sensor configurations that provide ultranarrow superhigh-Q resonances associated with the higher harmonics of the vibrational transitions of the organic molecules of NMA. In contrast to fundamental vibrations that have rather good SNR, but lie in the mid-IR, higher harmonics emerge in the NIR region, but have very low SNR. Therefore, the overtones are challenging to detect.

In the proposed PC nanostructures, we take advantage of the superhigh-Q modes in PC-based structures and MO effects and show the detectability of NMA molecules. By exciting the quasi-surface modes, well known for their extreme sensitivity to the materials' properties, the weak absorption peaks corresponding to the higher harmonics of the N-H vibrational transitions can be efficiently detected. We study both magnetic and nonmagnetic PC nanostructure sensors. The main advantage of the nonmagnetic PC nanostructure sensor is the small number of the layers in the PC structure. The design presented in this paper contains just four pairs of the dielectric layers and one additional Si layer. In the presence of NMA molecules in analyte, the reflectance spectrum of the proposed nonmagnetic PC nanostructure demonstrates an unambiguous change of profile that can be easily detected in experiment. Moreover, the magnetic PC nanostructure opens the possibility to detect the presence of NMA molecules in analyte with even greater precision.

Magnetic sensing demonstrates several orders of magnitude higher sensitivity as compared to the nonmagnetic sensing due to the measurements of superhigh-Q MO resonances. It is important that not only does the Q factor of the resonance increase, but so does the magnitude of the measured value (i.e., TMOKE instead of R), which makes the proposed structure very promising for vibrational overtone sensing applications. It should be noted that this sensor requires rather accurate fabrication. Specifically, the fabrication tolerances of the layer thicknesses should be around 2 nm to provide such sharp and deep resonances that are only 10% worse than in an ideal case (Fig. 4). The tolerance of the structure to the deviations of the PC parameters is described in detail in Appendix A. However such fabrication restriction is quite accessible with present technologies of thin-film deposition [28–30,35–37].

It is important to note that the MO sensing configuration has the advantages of significantly improved SNR. Also, since the measurement of the relative variation of the reflectance does not require precise normalization of the intensity, it also helps to avoid any spurious interference present in the experimental scheme. This is very important for the development of highly sensitive spectroscopic tools based on high-Q magnetophotonic sensors of high SNR.

Therefore, the presented sensing structure allows for the precise detection of small absorption peaks of the material in the NIR, which are the "fingerprints" corresponding to certain molecules and bounds.

6. MATERIALS AND METHODS

The PCs' structures are designed to provide an ultranarrow resonance of quasi-surface electromagnetic wave in accordance with the impedance approach described, for instance, in Refs. [35,38]. The parameters of the PC are chosen to provide the same optical impedances for both sides of the PC/analyte interface. This method is based on Fresnel formulas and gives a recursive analytical formula, so it allows for the direct numerical calculation of optical properties of the structure, including far-field (e.g., reflectance) and near-field (electromagnetic field distribution) response. The details can be found in Appendix D.

We design the nonmagnetic PC nanostructure [see Fig. 2(a)], which is composed of four pairs of Si/Si_3N_4 layers. The thickness of the Si layers in PC is 135 nm, and the Si_3N_4 layers are 222-nm-thick each. Besides that, there is a bottom Si layer with the thickness of $h = 260$ nm between PC and the

analyte. To introduce the s-polarized light into the PC structure at the required incidence angle, one can use an equilateral Si prism with the base angles of around 27.1°, depending on the angular position of the resonance in the reflection spectra.

In addition, we propose a magnetic PC nanostructure composed of 20 pairs of Ta_2O_5/Si layers and an additional magnetic layer of cerium-substituted yttrium iron garnet (CeYIG). The order and thickness of the layers have been optimized to achieve minimal values of both reflection coefficient R and impedance Z of the structure. The best results were obtained for the PC nanostructure given in Fig. 7 (in Appendix C). 255-nm-thick Ta_2O_5 layers alternate with 373-nm-thick Si layers. The CeYIG film should be 50 nm thick.

The fabrication technologies required for making the proposed PC nanostructures are well developed and widely applied. For instance, similar PC structures have been experimentally studied in Refs. [28–33,35–37], to mention just a few. Note that the typical fabrication precision is about 0.5 nm [35–37], so the fabrication tolerance of 2 nm required for the proposed PC nanostructures can be easily provided.

The refractive indices of the materials at the wavelength 1.495 μm were taken as the following: $n_{Si} = 3.4804$ at $T = 293$ K [39], $n_{Si_3N_4} = 1.9978$ [40], $n_{Ta_2O_5} = 2.0591$ [41], $n_{TiO_2} = 2.4548$ [42], $n_{NMA} = 1.5712$ and $n''_{NMA} = 10^{-4}$ [4,7], $n_{CeYIG} = 4.95$, and gyration $g_{CeYIG} = 10^{-2}$ (see, for instance, Ref. [43]).

APPENDIX A: TOLERANCE TO THE LAYER THICKNESS AND REFRACTIVE INDEX

The high-Q resonance in the proposed structures is very sensitive to the deviations of the widths and refractive indices of the layers. In order to study the structure tolerance in detail, we have performed the calculations where the thicknesses w_j and the refractive indices n_j of the structure layers were disturbed by randomly distributed values of the certain magnitude $w_j + \delta w_j$ and $n_j + \delta n_j$. Figure 4 shows the relative magnitude I/I_0 of the quasi-surface wave intensity in the disturbed structure normalized on the surface wave intensity in the nondisturbed structure I_0 with respect to the magnitude of δw_j and δn_j averaged over 100 randomly generated deviations.

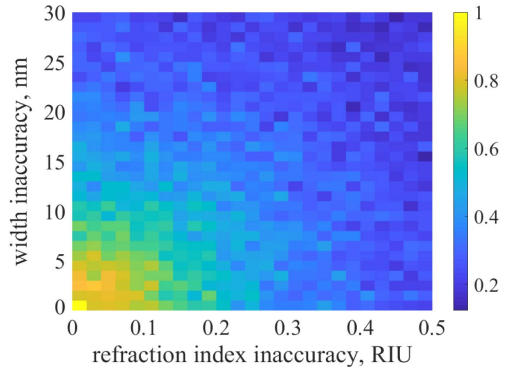

Fig. 4. Relative magnitude I/I_0 of the quasi-surface wave intensity in the disturbed structure normalized on the surface wave intensity in the nondisturbed structure I_0, with respect to the magnitude of δw_j in nanometers and δn_j in refractive index units (RIU) deviations from the designed values averaged over 100 randomly generated deviations.

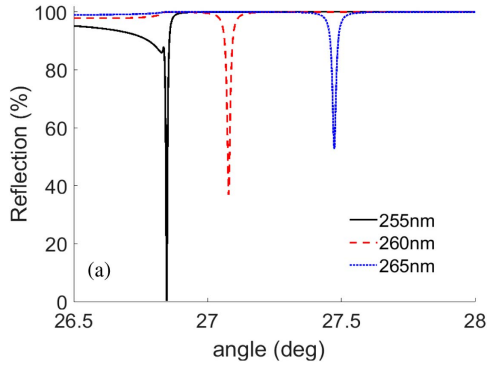

Fig. 5. Normalized reflectance (in percents of light energy reflected by the structure normalized to the incident energy) versus angle of incidence (degrees) of superhigh Q resonance at the wavelength of the incident light 1.495 μm. Resonant curves corresponding to different thicknesses of the bottom Si layer, 255 nm (black solid curve), 260 nm (red dashed curve), and 265 nm (blue dotted curve).

According to Fig. 4, the accuracy of the layer deposition $\delta w_j < 10$ nm and $\delta n_j < 0.15$ RIU leads to less than twice the decrease in the quasi-surface wave magnitude compared to the ideal case. At the same time, the less than 2 nm deviation of the layer widths and less than 0.05 RIU deviation of the refractive indices diminish the mode amplitude by only 10% compared to the ideal structure.

In Fig. 5, we plot the evolution of the resonances as a function of the bottom Si layer thickness h, which is a guiding layer for quasi-surface waves. The narrowest and deepest resonance is provided by the thinnest Si layer, $h = 255$ nm. This occurs at around 26.8° (solid black curve). Even though the thicker layers of $h = 260$ nm and $h = 265$ nm do not provide such narrow resonances, the corresponding dips in the reflection spectra are still sufficient for the effective detection of NMA molecules. Moreover, with the growth of h, the angular position of the resonance moves toward the larger values of the incident angle. Naturally, the Si layer thickness of 255 nm is preferable, but in many cases the standard accuracy of the fabrication admits the thickness tolerances of about a few nanometers. Thus, it is crucial to guarantee that the proposed design of the PC nanostructure still has high-Q resonances even in the case of a small deviation dictated by the design thickness.

APPENDIX B: ANGULAR SPECTRA FOR THE PC-BASED STRUCTURE WITH QUASI-GUIDED MODES

There are two approaches to obtaining angular spectra in sensing measurements. The first one is based on utilization of the collimated light with the angular width much smaller than the dip width, 0.01°, namely, in the case of PC-based ultrahigh-Q structures. The angle of incidence is varied by the mechanical motion of the sample with a prism and the corresponding motion of the light detector. This scheme would provide the reflectance curves shown in Fig. 6 for the cases of absorbing and "nonabsorbing" NMA material.

The second approach is utilization of a light beam with higher angular width, focused at the sample surface via the lens. After

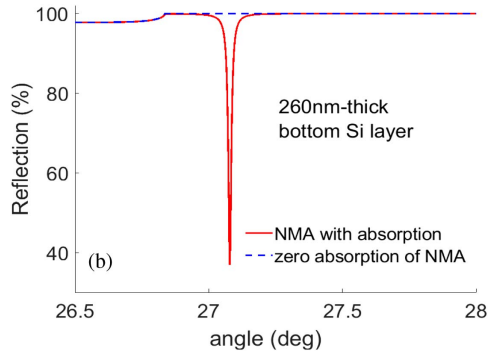

Fig. 6. Normalized reflectance (in percents of light energy reflected by the structure normalized to the incident energy) versus angle of incidence (degrees) of superhigh Q resonance at the wavelength of the incident light 1.495 μm. Resonant curves in the cases of absorbing ($n'' = 10^{-4}$, red solid curve) and nonabsorbing ($n'' = 0$, blue dashed curve) analyte material with the same real part of the refractive index.

reflection from the sample, the light is collimated via the prism and detected by a complementary metal-oxide-semiconductor matrix so that each pixel corresponds to a certain angle of incidence. This approach allows for the simultaneous measurement of the angular spectra. However, it should be noted that the interference of the light, reflected directly from the sample, and the light, transferred to the waveguide mode and coupled back, will take place. This will cause the typical interference pattern in angular spectrum of the reflected light (similar to the one observed in Ref. [27]); however, the excitation of long-range propagating mode will still result in the dip corresponding to its absorption.

APPENDIX C: SCHEME OF SENSING WITH MAGNETIC PC-BASED STRUCTURE WITH QUASI-GUIDED MODES

In Fig. 7, one can see the scheme of the proposed magnetic PC nanostructure for the weak absorption peak sensing addressed in Section 4. The PC nanostructure consists of 20 pairs of Ta_2O_5 (255 nm)/Si (373 nm) layers and is terminated with a magnetic CeYIG layer, deposited to provide MO response. The structure under consideration is placed inside the reversible magnetic field H directed along the plane of the PC layers and orthogonally to the wave vector of the incident light. The incident light is p-polarized to provide the excitation of the TM mode inside the nanostructure. The reflected light is detected on the other side facet of the prism.

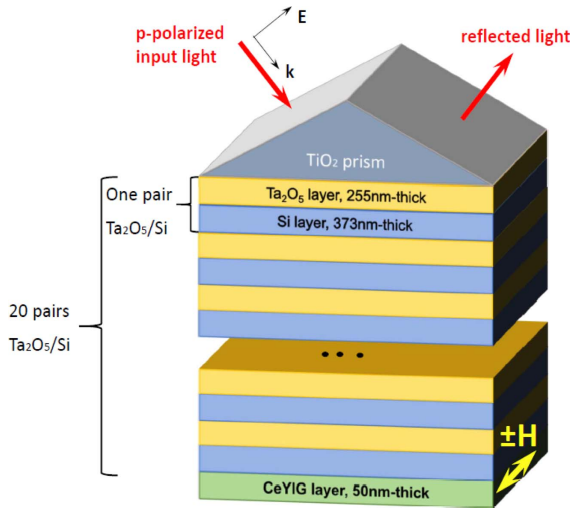

Fig. 7. Scheme of the magnetic PC nanostructure in the external magnetic field H. Input and reflected light at 1.495 μm is shown with red arrows.

APPENDIX D: IMPEDANCE APPROACH FOR MULTILAYERED STRUCTURES

Multilayered structures allow for the analytical description of their optical properties based on the well-known plane-wave solution of Maxwell equations and Fresnel coefficients. Many methods were elaborated for the multilayered structure description; the most famous among them is the well-known scattering matrix approach.

However, for the case of the structure where p- and s-incident polarizations produce some eigenmodes, the most convenient is the impedance approach that was proposed and described in detail in Ref. [38]. It relies on the calculation of the "impedance" of the medium $Z = E_{\tan}/H_{\tan}$, and the key characteristic of the jth layer of width d_j is its input impedance,

$$Z_j^{\text{into}} = Z_j \cdot \frac{Z_{j+1}^{\text{into}} - iZ_j \tan(\alpha_j)}{Z_j - iZ_{j+1}^{\text{into}} \tan(\alpha_j)},$$

where $\alpha_j = k_{zj} d_j$. On the one hand, such a description allows for the calculation of the optical properties: transmission, reflection, and electromagnetic field distribution inside of a structure directly from Z_j^{into} values (see Ref. [38] for formulas). On the other hand, it allows for the analytical description of the conditions under which surface and quasi-surface waves exist at any interface inside of the structure. It has been shown [38] that the most general condition for the surface wave excitation in terms of the impedances is

$$Z_{\text{left}} + Z_{\text{right}} = 0,$$

so that the parameters of the PC-based structures could be tuned to provide the quasi-surface wave resonance at the desired wavelength.

Note that the structure is considered to be infinite in the xy directions, and the incident light is considered in the form of the plane monochromatic wave.

Funding. Israeli Innovation Authority-Kamin Program; (62045 Year 2); Russian Foundation for Basic Research (19-02-00856_a); Russian Science Foundation (18-72-00233).

Acknowledgment. V. I. B. and O. V. B. acknowledge support from the Foundation for the Advancement of Theoretical Physics BASIS.

REFERENCES

1. W. S. Struve, *Fundamentals of Molecular Spectroscopy* (Wiley, 1989).

2. R. Adato and H. Altug, "*In-situ* ultra-sensitive infrared absorption spectroscopy of biomolecule interactions in real time with plasmonic nanoantennas," Nat. Commun. **4**, 2154 (2013).
3. D. Dregely, F. Neubrech, H. Duan, R. Vogelgesang, and H. Giessen, "Vibrational near-field mapping of planar and buried three-dimensional plasmonic nanostructures," Nat. Commun. **4**, 2237 (2013).
4. A. Karabchevsky and A. V. Kavokin, "Giant absorption of light by molecular vibrations on a chip," Sci. Rep. **6**, 21201 (2016).
5. A. Karabchevsky, A. Katiyi, M. I. M. Abdul Khudus, and A. V. Kavokin, "Tuning the near-infrared absorption of aromatic amines with photonic microfibers sculptured gold nanoparticles," ACS Photon. **5**, 2200–2207 (2018).
6. A. Katiyi and A. Karabchevsky, "Si nanostrip rib-waveguide for on-chip broadband molecular overtone spectroscopy in near-infrared," ACS Sens. **3**, 618–623 (2018).
7. A. Katiyi and A. Karabchevsky, "Figure of merit of all-dielectric waveguide structures for absorption overtone spectroscopy," J. Lightwave Technol. **35**, 2902–2908 (2017).
8. A. Karabchevsky and A. Shalabney, "Strong interaction of molecular vibrational overtones with near-guided surface plasmon polariton," Proc. SPIE **9899**, 98991T (2016).
9. D. R. Dadadzhanov, T. A. Vartanyan, and A. Karabchevsky, "Differential extinction of vibrational molecular overtone transitions with gold nanorods and its role in surface enhanced near-IR absorption (SENIRA)," Opt. Express **27**, 29471–29478 (2019).
10. A. V. Kabashin, P. Evans, S. Pastkovsky, W. Hendren, G. A. Wurtz, R. Atkinson, R. Pollard, V. A. Podolskiy, and A. V. Zayats, "Plasmonic nanorod metamaterials for biosensing," Nat. Mater. **8**, 867–871 (2009).
11. D. Garoli, E. Calandrini, G. Giovannini, A. Hubarevich, V. Caligiuri, and F. De Angelis, "Nanoporous gold metamaterials for high sensitivity plasmonic sensing," Nanoscale Horiz. **4**, 1153–1157 (2019).
12. K. V. Sreekanth, Y. Alapan, M. Elkabbash, E. Ilker, M. Hinczewski, U. A. Gurkan, A. De Luca, and G. Strangi, "Extreme sensitivity biosensing platform based on hyperbolic metamaterials," Nat. Mater. **15**, 621–627 (2016).
13. J. Homola, "Surface plasmon resonance sensors for detection of chemical and biological species," Chem. Rev. **108**, 462–493 (2008).
14. J. N. Anker, W. P. Hall, O. Lyandres, N. C. Shah, J. Zhao, and R. P. Van Duyne, "Biosensing with plasmonic nanosensors," Nat. Mater. **7**, 442–453 (2008).
15. N. E. Khokhlov, D. O. Ignatyeva, and V. I. Belotelov, "Plasmonic pulse shaping and velocity control via photoexcitation of electrons in a gold film," Opt. Express **22**, 28019–28026 (2014).
16. D. O. Ignatyeva and A. P. Sukhorukov, "Plasmon beams interaction at interface between metal and dielectric with saturable Kerr nonlinearity," Appl. Phys. A **109**, 813–818 (2012).
17. D. O. Ignatyeva and A. P. Sukhorukov, "Femtosecond-pulse control in nonlinear plasmonic systems," Phys. Rev. A **89**, 013850 (2014).
18. O. Borovkova, A. Kalish, and V. Belotelov, "Transverse magneto-optical Kerr effect in active magneto-plasmonic structures," Opt. Lett. **41**, 4593–4596 (2016).
19. O. V. Borovkova, H. Hashim, M. A. Kozhaev, S. A. Dagesyan, A. Chakravarty, M. Levy, and V. I. Belotelov, "TMOKE as efficient tool for the magneto-optic analysis of ultra-thin magnetic films," Appl. Phys. Lett. **112**, 063101 (2018).
20. O. V. Borovkova, F. Spitzer, V. I. Belotelov, I. A. Akimov, A. N. Poddubny, G. Karczewski, M. Wiater, T. Wojtowicz, A. K. Zvezdin, D. R. Yakovlev, and M. Bayer, "Transverse magneto-optical Kerr effect at narrow optical resonances," Nanophotonics **8**, 287–296 (2019).
21. M. Levy, O. V. Borovkova, C. Sheidler, B. Blasiola, D. Karki, F. Jomard, M. A. Kozhaev, E. Popova, N. Keller, and V. I. Belotelov, "Faraday rotation in iron garnet films beyond elemental substitutions," Optica **6**, 642–646 (2019).
22. C. A. Herreño-Fierro, E. J. Patiño, G. Armelles, and A. Cebollada, "Surface sensitivity of optical and magneto-optical and ellipsometric properties in magnetoplasmonic nanodisks," Appl. Phys. Lett. **108**, 021109 (2016).
23. B. Sepúlveda, A. Calle, L. M. Lechuga, and G. Armelles, "Highly sensitive detection of biomolecules with the magneto-optic surface-plasmon-resonance sensor," Opt. Lett. **31**, 1085–1087 (2006).
24. D. Regatos, D. Fariña, A. Calle, A. Cebollada, B. Sepúlveda, G. Armelles, and L. M. Lechuga, "Au/Fe/Au multilayer transducers for magneto-optic surface plasmon resonance sensing," J. Appl. Phys. **108**, 054502 (2010).
25. N. Maccaferri, K. E. Gregorczyk, T. A. G. de Oliveira, M. Kataja, S. van Dijken, Z. Pirzadeh, A. Dmitriev, J. Åkerman, M. Knez, and P. Vavassori, "Ultrasensitive and label-free molecular-level detection enabled by light phase control in magnetoplasmonic nanoantennas," Nat. Commun. **6**, 6150 (2015).
26. S. David, C. Polonschii, C. Luculescu, M. Gheorghiu, S. Gáspár, and E. Gheorghiu, "Magneto-plasmonic biosensor with enhanced analytical response and stability," Biosens. Bioelectron. **63**, 525–532 (2015).
27. M. G. Manera, E. Ferreiro-Vila, J. M. Garcia-Martin, A. Garcia-Martin, and R. Rella, "Enhanced antibody recognition with a magneto-optic surface plasmon resonance (MO-SPR) sensor," Biosens. Bioelectron. **58**, 114–120 (2014).
28. V. N. Konopsky and E. V. Alieva, "Photonic crystal surface waves for optical biosensors," Anal. Chem. **79**, 4729–4735 (2007).
29. D. O. Ignatyeva, P. O. Kapralov, G. A. Knyazev, S. K. Sekatskii, G. Dietler, M. Nur-E-Alam, M. Vasiliev, K. Alameh, and V. I. Belotelov, "High-*Q* surface modes in photonic crystal/iron garnet film heterostructures for sensor applications," JETP Lett. **104**, 679–684 (2016).
30. D. O. Ignatyeva, G. A. Knyazev, P. O. Kapralov, G. Dietler, S. K. Sekatskii, and V. I. Belotelov, "Magneto-optical plasmonic heterostructure with ultranarrow resonance for sensing applications," Sci. Rep. **6**, 28077 (2016).
31. J. Qin, Y. Zhang, X. Liang, C. Liu, C. Wang, T. Kang, H. Lu, L. S. Zhang, P. Zhou, X. Wang, B. Peng, J. Hu, L. Deng, and L. Bi, "Ultrahigh figure-of-merit in metal-insulator-metal magnetoplasmonic sensors using low loss magneto-optical oxide thin films," ACS Photon. **4**, 1403–1412 (2017).
32. A. M. Merzlikin, E. V. Kuznetsov, and A. V. Baryshev, "Magneto-optical device based on polarization sensitivity for perspective biosensing applications," IEEE Sens. J. **18**, 5732–5738 (2018).
33. B. Caballero, A. Garcia-Martin, and J. C. Cuevas, "Hybrid magnetoplasmonic crystal boost performance of nanohole arrays as plasmonic sensors," ACS Photon. **3**, 203–208 (2016).
34. A. Zvezdin and V. Kotov, *Modern Magnetooptics and Magnetooptical Materials* (IOP, 1997).
35. S. K. Sekatskii, S. Smirnov, G. Dietler, M. N. E. Alam, M. Vasiliev, and K. Alameh, "Photonic crystal-supported long-range surface plasmon-polaritons propagating along high-quality silver nanofilms," Appl. Sci. **8**, 248 (2018).
36. V. N. Konopsky, T. Karakouz, E. V. Alieva, C. Vicario, S. K. Sekatskii, and G. Dietler, "Photonic crystal biosensor based on optical surface waves," Sensors **13**, 2566–2578 (2013).
37. E. Rostova, C. B. Diba, G. Dietler, and S. Sekatskii, "Label-free optical biosensor based on photonic crystal reveals binding kinetics of antibodies to living bacterial cells *E. coli*," Biosensors **6**, 52 (2016).
38. V. N. Konopsky, "Plasmon-polariton waves in nanofilms on one-dimensional photonic crystal surfaces," New J. Phys. **12**, 093006 (2010).
39. H. H. Li, "Refractive index of silicon and germanium and its wavelength and temperature derivatives," J. Phys. Chem. Ref. Data **9**, 561–658 (1980).
40. K. Luke, Y. Okawachi, M. R. E. Lamont, A. L. Gaeta, and M. Lipson, "Broadband mid-infrared frequency comb generation in a Si_3N_4 microresonator," Opt. Lett. **40**, 4823–4826 (2015).
41. T. J. Bright, J. I. Watjen, Z. M. Zhang, C. Muratore, A. A. Voevodin, D. I. Koukis, D. B. Tanner, and D. J. Arenas, "Infrared optical properties of amorphous and nanocrystalline Ta_2O_5 thin films," J. Appl. Phys. **114**, 083515 (2013).
42. J. R. DeVore, "Refractive indices of rutile and sphalerite," J. Opt. Soc. Am. **41**, 416–419 (1951).
43. S. Higuchi, Y. Furukawa, S. Takekawa, O. Kamada, K. Kitamura, and K. Uyeda, "Magnetooptical properties of cerium-substituted yttrium iron garnet single crystals for magnetic-field sensor," Sens. Actuators A Phys. **105**, 293–296 (2003).